RESEARCH ARTICLE

Quantitative proteomic analysis of G-protein signalling in *Stagonospora nodorum* using isobaric tags for relative and absolute quantification

Tammy Casey[1,2*], *Peter S. Solomon*[3*], *Scott Bringans*[1], *Kar-Chun Tan*[4], *Richard P. Oliver*[4] *and Richard Lipscombe*[1,2]

[1] Proteomics International, Perth, WA, Australia
[2] Centre for Food and Genomic Medicine, Perth, WA, Australia
[3] Plant Cell Biology, Research School of Biology, The Australian National University, Canberra, ACT, Australia
[4] Australian Centre for Necrotrophic Fungal Pathogens, SABC, DHS, Murdoch University, Perth, WA, Australia

Received: July 3, 2010
Revised: September 23, 2009
Accepted: September 29, 2009

The G protein α-subunit (*Gna1*) in the wheat pathogen *Stagonospora nodorum* has previously been shown to be a critical controlling element in disease ontogeny. In this study, iTRAQ and 2-D LC MALDI-MS/MS have been used to characterise protein expression changes in the *S. nodorum gna1* strain *versus* the SN15 wild-type. A total of 1336 proteins were identified. The abundance of 49 proteins was significantly altered in the *gna1* strain compared with the wild-type. Gna1 was identified as having a significant regulatory role on primary metabolic pathways, particularly those concerned with NADPH synthesis or consumption. Mannitol dehydrogenase was up-regulated in the *gna1* strain while mannitol 1-phosphate dehydrogenase was down-regulated providing direct evidence of *Gna1* regulation over this enigmatic pathway. Enzymatic analysis and growth assays confirmed this regulatory role. Several novel hypothetical proteins previously associated with stress and pathogen responses were identified as positively regulated by Gna1. A short-chain dehydrogenase (Sch3) was also significantly less abundant in the *gna1* strains. Sch3 was further characterised by gene disruption in *S. nodorum* by homologous recombination. Functional characterisation of the *sch3* strains revealed their inability to sporulate *in planta* providing a further link to *Gna1* signalling and asexual reproduction. These data add significantly to the identification of the regulatory targets of *Gna1* signalling in *S. nodorum* and have demonstrated the utility of iTRAQ in dissecting signal transduction pathways.

Keywords:
G-protein / iTRAQ / Mannitol / Microbiology / Signal transduction

1 Introduction

The significant role of G-protein signalling for the pathogenicity of phytopathogenic fungi has long been established. The α subunit(s) of the heterotrimeric G-protein in particular has received considerable attention with its role as a dominant controlling element in pathogenicity and a multitude of other phenotypes confirmed [1–9]. Gα signalling is presumed to control these processes *via* various signalling pathways but the nature of the downstream effectors is not well understood. Disruption of a Gα gene was used to study virulence-associated development in the pathogen *Stagonospora nodorum* [10, 11]. *S. nodorum* is a necrotrophic dothideomycete phytopathogen that is the causal agent of leaf and glume blotch on wheat and is responsible for $60 M (AUD) of crop loss in Australia each

Correspondence: Dr. Peter S. Solomon, Plant Cell Biology, Building 46, Research School of Biology, The Australian National University, Canberra, ACT, Australia
E-mail: peter.solomon@anu.edu.au
Fax: +61-2-6125-4331

Abbreviations: DOPA, dihydroxyphenylalanine; **EF,** error factor; **KO,** knockout; **MM,** minimal media; **PPP,** pentose phosphate pathway; **TEAB,** triethylammonium bicarbonate; **UTR,** untranslated region

*These authors contributed equally to this work.

year [12, 13]. Strains of *S. nodorum* harbouring an impaired Gα gene exhibited various phenotypes including reduced pathogenicity, a failure to melanise, an inability to sporulate and reduced extracellular enzyme production.

Studies exploiting functional genomics approaches to better understand the downstream effectors of Gα signalling are emerging. Transcriptomics has been used to elucidate targets of Gα subunit signalling in the grey mold *Botrytis cinerea* and the chestnut blight fungus *Cryphonectria parasitica*. These studies have shown signalling regulation of *B. cinerea* genes with putative roles in secondary metabolism, proteolysis and carbohydrate metabolism genes [14] and hypovirus-responsive genes in *C. parasitica* [15], respectively.

However, it is now well understood that gene expression does not necessarily correlate with protein abundance. A key study by Gygi *et al.* [16] demonstrated that abundance of approximately only half of the transcripts in *Saccharomyces cerevisiae* correlated with protein levels, suggesting that it would be difficult to dissect phenotypes on the basis of gene expression data alone. A previous study by Tan *et al.* [17] identified a similar pattern of transcript/protein abundance in *S. nodorum* [11], confirming that protein expression levels cannot be predicted from quantitative mRNA data.

Proteomic approaches have been exploited over the last decade to dissect plant-pathogen interactions, including the study of plant responsive proteins, morphogenesis and stress response [18]. Proteomics has also recently been used to identify the targets of G-protein signalling. Gel-based proteomics studies on mutants of *S. nodorum* harbouring a disrupted Gα subunit (*Gna1*) have revealed novel features of this pathogen including the involvement of the short-chain dehydrogenase Sch1 in asexual sporulation and mycotoxin production [17, 19].

Over the last decade gel-free proteomics techniques (LC-MS/MS or LC-LC-MS/MS) have emerged as complementary techniques to existing gel-based 2-D PAGE. These techniques reportedly overcome many of the limitations of 2-D PAGE including the detection of low-abundance proteins and also proteins of extreme M_r and/or p*I* [20]. Gel-free proteomics techniques are also more amenable to quantitative techniques such as isotope labelling, iCAT and iTRAQ [21]. In this study, we re-analyse the proteomes of a wild-type *S. nodorum* strain and the *Gna1* mutant strain using 2-D LC-MALDI-MS/MS and iTRAQ to shed further light on the targets of Gna1 signalling in *S. nodorum*. The MALDI-MS/MS mass spectrometer, when compared with ion trap electrospray-based systems has the advantages of increased resolution as a TOF instrument, the ability to re-analyse archived samples and its relative insensitivity to ion suppression agents [22, 23]. Amongst the proteins altered in this study were two involved in mannitol metabolism. Mannitol is a highly abundant metabolite in filamentous fungi and previous studies in *S. nodorum* have highlighted the critical role of mannitol metabolism in asexual sporulation [24, 25].

2 Materials and methods

2.1 Growth and maintenance of *S. nodorum*

S. nodorum SN15 wild-type (Department of Agriculture, Western Australia) and the *gna1* strain carrying a disrupted *Gna1* (Genbank accession number EAT82421) were used in this study. All strains were maintained on CZV8CS agar as previously described [1]. For proteomic analysis, 100 mg of fungal mycelia were inoculated into minimal medium (MM) broth supplemented with 25 mM glucose as the sole carbon source. The fungal strains were grown to an exponential vegetative growth-phase by incubation at 22°C with shaking at 150 rpm for 3 days. Vegetative mycelia were harvested *via* cheesecloth filtration and freeze-dried overnight.

2.2 Protein extraction

Soluble intracellular proteins were extracted from freeze-dried mycelia as previously described [17]. Briefly, freeze-dried mycelia were mechanically broken with a cooled mortar and pestle and proteins were solubilised with 10 mM Tris-Cl (pH 7.5). The crude homogenate was collected and centrifuged at $20\,000 \times g$ for 15 min at 4°C. The resulting supernatant was retained and treated with nucleases to remove nucleic acids. All protein samples were checked *via* SDS-PAGE to ensure that proteolysis was minimal during sample preparation (data not shown).

2.3 Sample preparation and iTRAQ labelling

Proteins from SN15 and *gna1* strains were precipitated individually by adding five volumes of acetone, incubating for 1 h at −20°C and pulse centrifuging for 5–10 s. The protein pellets were re-suspended in 0.5 M triethylammonium bicarbonate (TEAB) (pH 8.5) before reduction and alkylation according to the iTRAQ protocol (Applied Biosystems, Foster City, CA, USA). Samples were centrifuged at $13\,000 \times g$ for 10 min at room temperature before the supernatant was removed and assayed for protein concentration (Bio-Rad protein assay kit, Hercules, CA, USA). A total of 55 μg of each sample was digested overnight with 5.5 μg trypsin at 37°C in 0.5 M TEAB. As part of the laboratory's operating procedures standards were digested concurrently to ensure tryptic digestion performance. Each digest was dried in a SpeedVac, re-suspended in 30 μL 0.5 M TEAB and labelled by adding iTRAQ reagents 114 and 116 to SN15 and SNGna35 samples, respectively. Excess iTRAQ reagent was quenched by adding 1 mL water, the samples were then combined, desalted on a Strata-X 33 μm polymeric reverse phase column (Phenomenex, Torrance, CA, USA) and dried. The entire experiment was performed in triplicate (including the generation of ground mycelia).

2.4 Strong cation exchange chromatography

Peptides were separated by strong cation exchange chromatography on an Agilent 1100 HPLC system (Agilent Technologies, Palo Alto, CA, USA) using a PolySulfoethyl column (4.6 × 100 mm, 5 μm, 300 Å, Nest Group, Southborough, MA, USA). Peptides were eluted with a linear gradients of Buffer B (1 M KCl, 10% ACN and 10 mM KH_2PO_4, pH 3) A total of 40 fractions were collected and pooled into eight fractions, desalted and dried.

2.5 Reverse phase nano-LC MALDI-MS/MS

Peptide fractions were separated on a C18 PepMap100, 3 μm column (LC Packings, Sunnyvale, CA, USA) with a gradient of ACN in 0.1% trifluoroacetic acid using the Ultimate 3000 nano HPLC system (LC Packings-Dionex, Sunnyvale, CA, USA). The eluent was mixed with matrix solution (5 mg/mL CHCA) and spotted onto a 384 well OptiTOF plate (Applied Biosystems, Framingham, MA, USA) using a Probot Micro Fraction Collector (LC Packings, San Francisco, CA, USA).

Peptides were analysed on a 4800 MALDI-TOF/TOF mass spectrometer (Applied Biosystems) operated in reflector positive mode. MS data were acquired over a mass range of 800–4000 *m/z* and for each spectrum a total of 400 shots were accumulated. A job-wide interpretation method selected the 20 most intense precursor ions above a signal/noise ratio of 20 from each spectrum for MS/MS acquisition but only in the spot where their intensity was at its peak. MS/MS spectra were acquired with 4000 laser shots *per* selected ion with a mass range of 60 to the precursor ion −20.

2.6 Data analysis

Protein identification and quantification were performed using ProteinPilot™ 2.0.1 Software (Applied Biosytems, Foster City, CA, USA). MS/MS spectra were searched against the *Stagonospora* genomic database. Search parameters were: Sample type, iTRAQ 4plex (peptide labelled); Cys alkylation, MMTS; Digestion, trypsin; Instrument, 4800; Special factors, none; Species, none; Quantitate tab, checked; ID focus, Biological modifications, Search effort, thorough; Detected protein threshold (unused ProtScore), 1.3 – which corresponds to proteins identified with >95% confidence.

For quantification analysis, each of the three biological replicates were analysed separately. Average protein ratios, *p*-values to indicate significant differential expression and error factors (EF) were calculated by the software. The EF indicates that the value for the average protein ratio is expected to be found between (reported ratio) × (EF) and (reported ratio)/(EF) 95% of the time (ProteinPilot™ Software Help). To be considered as being differentially expressed, proteins were required to have an EF < 2, contain at least two unique high confidence peptides (peptide confidence >90%) and have significantly different protein ratios (*gna1*:SN15) in two of the three biological replicates [26].

To estimate the false discovery rate, a decoy database search against a concatenated database containing forward and randomised entries of the *Stagonospora* genomic database was performed. The false discovery rate was estimated to be 6.3% and was calculated as follows (number of random hits/(total number of hits–number of random hits)) × 100 [27].

2.7 Construction of the *Sch3* gene knockout vector and transformation of *S. nodorum*

Sch3 was deleted by gene replacement with a phleomycin-resistant selectable marker construct. The 5′ and 3′ untranslated region (UTR) of *Sch3* was PCR amplified with the primer pairs 5′FwdKpnI-R637 (5′-GGTACCGAGCTATGGAACATGTACAGG-3′)/5′RevXhoI-R637 (5′-CTCGAGTGTTTGCGCTTCACTTGCTT-3′) and 3′ FwdBamHI-R637 (5′-GGATCCGTACAGTGGCTGAAGACTGA-3′)/3′RevNotI-R637 (5′-GCGGCCGCATGTAGTAATCATTTAGGTC-3′), respectively. Restriction sites were introduced into the primer sequences to facilitate cloning with the phleomycin selectable marker plasmid vector pBSK-phleo [28]. To achieve this, the 5′ *Sch3* UTR amplicon (663 bp) was introduced into *Kpn*I and *Xho*I sites of pBSK-phleo to give pBSK-phleo-5′Sch3. Following this, the 3′ *Sch3* UTR amplicon (798 bp) was cloned into *Bam*HI and *Not*I sites of pBSK-phleo-5′Sch3 to give the knockout vector pBSK-Sch3KO (KO, knockout). A 3.61 kb gene deletion KO construct was PCR-amplified from pBSK-Sch3KO using the primer pair R637FwdKO (5′-ATGGAACATGTACAGGGTGTCGC-3′) and R637RevKO (5′-GCAACAACACTGAACGTGCTCAA-3′) primers were used to amplify the KO construct for transformation.

Transformation of the *Sch3* deletion construct into *S. nodorum* was undertaken as previously described [29]. Homologous recombination of the deletion construct into the *S. nodorum* genome was checked by PCR using primers that spanned the flanking regions (R6375′KOScr 5′-GCAGATCTAGCGAAGTATGACGGG-3′; R6373′KOScr 5′-CGAGAAGGACAACATTGACTTTGGG-3′).

2.8 Enzyme assays

Mannitol dehydrogenase activity was assayed as previously described [30]. The reaction mixture contained 0.25 mM NADPH, 0.8 M fructose and protein extract. The volume was made up to 1 mL with 20 mM Tris-HCl (pH 7.5). One unit was defined as the enzyme activity needed to oxidise

1 μmol of NADPH *per* min at 30°C. Mannitol 1-phosphate dehydrogenase assay contained 0.25 mM NADH and 50 μL of protein extract in 50 mM Tris-HCl, pH 7.5, in a volume of 1 mL. The reaction was started with the addition of fructose 6-phosphate to a final concentration of 2 mM unless otherwise stated. One unit was defined as the enzyme activity needed to oxidise 1 μmol of NADH *per* min at 30°C. Total protein content was determined using the bicinchoninic acid technique as previously described [31].

3 Results and discussion

3.1 1336 unique proteins were identified in *S. nodorum*

Intracellular proteins from *S. nodorum* SN15 and *gna1* were extracted and digested with trypsin prior to iTRAQ analysis. Mass spectra from three biological replicates were analysed using ProteinPilot™ 2.0.1 Software. A total of 974, 922 and 910 proteins were identified with >95% confidence for each of the biological replicates from 20 294, 19 037 and 17 417 MS/MS spectra, respectively (Supporting Information Fig. 1). Overall, 1336 proteins were identified from 56 748 spectra. A total of 590 proteins were present in all three biological replicates with at least 671 proteins identified in two of the three biological replicates (Fig. 1). A total of 456 proteins were identified in a single biological replicate with 175, 131 and 150 proteins being unique to replicates 1, 2 and 3, respectively.

The intracellular proteomes of wild-type *S. nodorum* and the *gna1* mutant have been previously compared *via* a 2-D gel-based approach with a total of 475 unique intracellular protein spots being identified [17]. Not all the spots were analysed so the number of unique proteins was not determined. This study identified 1336 unique proteins adding further evidence to the idea that LC-based proteomics approaches are more sensitive than gel-based [32, 33]. However, it should be noted that the gel-based study used only 7 cm IPG strips and small gels and thus a direct comparison of the two techniques in this case would be difficult.

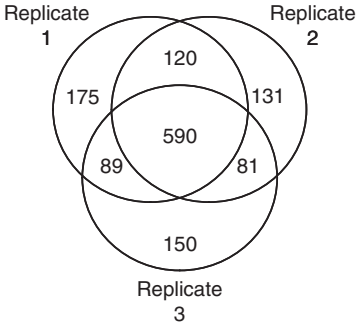

Figure 1. Protein identification by iTRAQ in three biological replicates.

Forty-nine proteins were present at statistically significant different levels in the *gna1* mutant strain; of these 25 proteins were present at higher levels, ranging from 1.3- to 2.7-fold increases (Table 1). The remaining 24 proteins were present at lower levels in the *gna1* strain with levels that were 1.3- to 4.8-fold lower than the SN15 strain. Representative spectra for peptides derived from SNOG_09682 and SNOG_08282 are displayed in Fig. 2, with peak areas of the signature ions 114.1 (SN15) and 116.1 (*gna1*) shown in the insets.

The results from the previous gel-based study identified seven proteins that were differentially abundant when comparing the wild-type and the *gna1* strain. Of these seven, the abundance of most correlated with the findings in this study but none were differentially abundant at a statistically significant level. This was not unexpected as LC-based and gel-based proteomics techniques are complementary techniques that will resolve and detect unique proteins as well as a common pool [34]. The growth conditions between the two studies also varied with 30 g/L glucose used for fungal growth in the gel-based approach and 5 g/L used in this study. One particular protein of significance was SNOG_10217 (Sch1), a short chain dehydrogenase previously shown to be required for sporulation in *S. nodorum* [17]. The gel-based approach revealed Sch1 was significantly less abundant in the *gna1* strain compared with the wild-type. A strong down-regulation trend for Sch1 in *gna1* was observed in this study even though the EF exceeded the maximum limit of two in each of the replicates.

3.2 Gna1 regulates mannitol metabolism

The most up-regulated protein in the *gna1* strain was mannitol dehydrogenase (Mdh1) while mannitol 1-phosphate dehydrogenase (Mpd1) was significantly less abundant in the mutant. Enzymatic analysis of both Mdh1 and Mpd1 were conducted to confirm the differential trend observed in protein abundances (Table 2). Mpd1 enzyme activity was reduced in the *gna1* strain while Mdh1 appeared significantly increased. The activities of these two enzymes were also examined *in planta*. The *gna1* strain is able to colonise wheat leaves, albeit slowly, but is unable to sporulate. Neither Mdh1 nor Mpd1 activities were detected in uninfected leaves (data not shown). This was not unexpected as there is no evidence to date of wheat metabolising mannitol. The specific activities of Mpd1 and Mdh1 *in planta* correlated with those observed *in vitro*. The Mdh1 activity was higher in the *gna1* strain during both the vegetative growth and sporulation stages of the infection cycle. Mpd1 activity was higher than Mdh1 during both stages of growth but was significantly lower in *gna1* compared with the wild-type strain, further supporting the claim that *Gna1* is a positive regulator of Mpd1 activity.

The ability of the *gna1* strain to metabolise mannitol was also examined. Growth assays on MM agar plates supplemented with different carbon sources were under-

Table 1. List of proteins identified as being significantly differential abundant when comparing *S. nodorum* SN15 and *gna1*

SNOG	Description	Fold change
SNOG_15488.2	Mannitol dehydrogenase	2.7±0f.3 (3)
SNOG_05229.2	$NADP^+$-specific glutamate dehydrogenase	2.5+0.5 (3)
SNOG_09682.2	Transaldolase	2.2+0.1 (3)
SNOG_08840.2	GMP synthase	2.1+1.2 (2)
SNOG_00877.2	Molecular chaperone	2.1+0.2 (3)
SNOG_15418.2	Farnesyl pyrophosphate synthetase	2.1+0.1 (2)
SNOG_15879.2	6-Phosphogluconate dehydrogenase	2.1±0.0 (2)
SNOG_06833.2	ATP citrate lyase	2.0+0.4 (2)
SNOG_10083.2	Transketolase	1.9+0.3 (2)
SNOG_10980.2	Glutamyl-tRNA synthetase	1.9+0.2 (2)
SNOG_01247.2	Hypothetical protein	1.8+0.5 (2)
SNOG_09416.2	Glucose-6-phosphate 1-dehydrogenase	1.8+0.3 (2)
SNOG_13188.2	Importin β-4	1.8+0.3 (2)
SNOG_10204.2	Inositol-3-phosphate synthase	1.8+0.2 (3)
SNOG_01742.2	Citrate synthase	1.8+0.1 (3)
SNOG_08437.2	Phosphoglucomutase	1.7+0.4 (2)
SNOG_03634.2	14-3-3 family protein	1.7+0.4 (2)
SNOG_02707.2	Dihydrolipoamide dehydrogenase	1.7+0.2 (3)
SNOG_14060.2	Prolyl-tRNA synthetase	1.7+0.1 (2)
SNOG_04804.2	Methionine synthase	1.6+0.3 (2)
SNOG_12730.2	Unknown	1.6+0.2 (3)
SNOG_05639.2	Peptidyl-prolyl *cis-trans* isomerase	1.6+0.2 (2)
SNOG_09984.2	Translation initiation factor 4b	1.5+0.0 (2)
SNOG_14322.2	Heat shock 70 kda protein	1.4+0.0 (2)
SNOG_15777.2	Phosphoglycerate mutase	1.3+0.0 (2)
SNOG_05888.2	Kinesin k39	−1.3±0.0 (2)
SNOG_04844.2	Hypothetical protein	−1.3±0.1 (2)
SNOG_13840.2	Bifunctional catalase-peroxidase cat2	−1.4±0.2 (2)
SNOG_07370.2	Small nuclear ribonucleoprotein	−1.5±0.2 (2)
SNOG_15469.2	Aldehyde reductase	−1.6±0.1 (2)
SNOG_05620.2	EF hand domain protein	−1.7±0.1 (2)
SNOG_12489.2	RNA binding effector protein	−1.8±0.3 (2)
SNOG_14994.2	Epoxide hydrolase cytoplasmic	−1.9±0.1 (2)
SNOG_02108.2	3-Deoxy-7-phosphoheptulonate synthase	−1.9±0.4 (2)
SNOG_04101.2	Actin-binding protein	−2.0±0.4 (2)
SNOG_09027.2	Malate NAD^+-dependent	−2.2±0.1 (2)
SNOG_14233.2	Hypothetical protein	−2.2±0.8 (2)
SNOG_02770.2	Hypothetical protein	−2.3±0.1 (2)
SNOG_15275.2	Hypothetical protein (Cyanovirin-n family protein domain)	−2.3±0.9 (2)
SNOG_12251.2	Protein disulfide isomerase	−2.4±0.4 (2)
SNOG_07136.2	Phosphoglycerate kinase	−2.5±0.2 (2)
SNOG_08267.2	Hypothetical protein	−2.8±0.2 (2)
SNOG_13050.2	Hypothetical protein	−3.2±1.2 (2)
SNOG_08282.2	Short chain oxidoreductase	−3.2±2.1 (2)
SNOG_12666.2	Mannitol-1-phosphate dehydrogenase	−3.3±0.4 (2)
SNOG_00806.2	RPEI repeat protein	−3.4±0.5 (2)
SNOG_04306.2	Hypothetical protein	−3.7±1.4 (2)
SNOG_02559.2	Actin cytoskeleton protein	−4.2±0.2 (3)
SNOG_11783.2	Glutaredoxin	−4.8±0.6 (2)

The abundance of proteins from the SN15 strain were used as the denominator to calculate the fold change (*i.e.* 2.7-fold refers to the protein being 2.7-fold more abundant in the *gna1* strain).

taken. The growth rate of the wild-type strain was comparable to that of the *gna1* strain using glucose as a sole carbon source (Fig. 3). The growth rate of the *gna1* strain was only 29% of the wild-type when mannitol was supplied as the sole carbon source. Both strains were also grown in MM containing both glucose and mannitol to determine if the decreased growth of the *gna1* strain on mannitol was due to impaired catabolism or toxicity. Levels of growth were restored for the *gna1* strain when grown on both carbon sources when compared with growth on glucose. These data

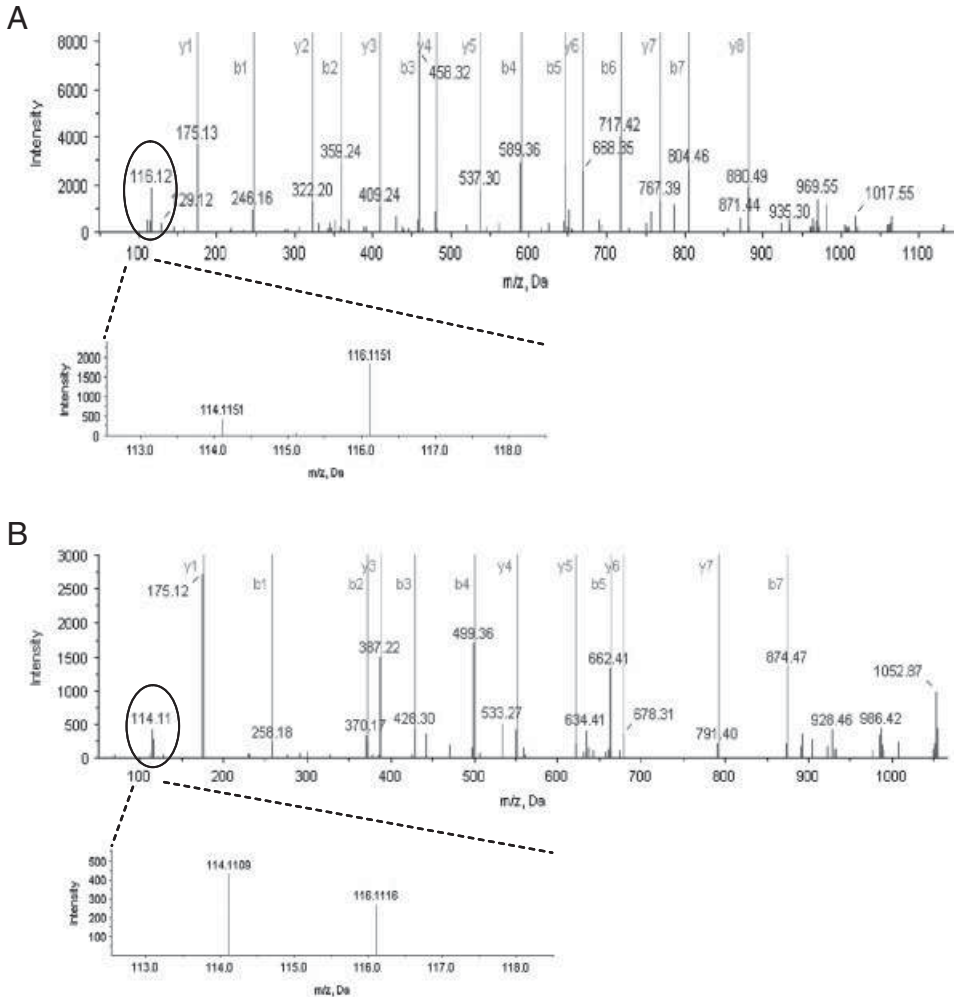

Figure 2. Representative MS/MS spectra of peptides derived from up-regulated SNOT_09682 (A) and down-regulated SNOT_08282 (B). SN15 wild-type and *gna1* mutant strains were labelled with iTRAQ reagents 114 and 116, respectively. (A) MS/MS spectra of TIVMGASFR from SNOT_09682; (B) MS/MS spectra of LLGAYPDR from SNOT_08282.

Table 2. Specific activities of Mdh1 and Mpd1 in *S. nodorum* wild-type and *gna1* strains during infection and also grown *in vitro*

	4 dpi *in planta*		8 dpi *in planta*		3 dpi *in vitro*	
	SN15	*gna1*	SN15	*gna1*	SN15	*gna1*
Mdh1	8.2±2.3	15.4±3.0	19.4±3.4	28.7±6.85	4.63±1.65	7.98±2.22
Mpd1	57.3±6.1	25.1±5.5	97.7±10.4	34.5±9.45	34.2±7.55	9.87±2.65

Measurements were taken on three biological replicates and the activities are expressed as mU/mg.

suggest that the *gna1* strain is impaired in its ability to metabolise mannitol and is consistent with metabolism occurring *via* Mpd1 (Fig. 4) [24, 25, 35]

Previous studies in *S. nodorum* have highlighted the critical role of mannitol metabolism in asexual sporulation [24, 25]. Mutants lacking Mpd1 were unable to sporulate while mutants lacking Mdh1 were unaffected. One of the many phenotypes of the *gna1* strain is its inability to asexually sporulate [1] and it is possible that this is due to reduced levels of Mpd1. Supplementation of growth media with mannitol did not restore sporulation, suggesting that the inability of the *gna1* strain to sporulate is not solely due to impaired mannitol metabolism. Previous studies have identified the short-chain dehydrogenase *Sch1* as being required for the maturation of immature pycnidia [17]. *Sch1* mutants were able to produce small immature pycnidia that lacked correct cellular structure (Supporting Information Fig. 2). In contrast, pycnidia are completely absent in the *Mpd1* and *Gna1* mutants, suggesting that mannitol is required for initiation of asexual sporulation and Sch1 is involved in subsequent maturation.

Heterotrimeric G-protein signalling and mannitol metabolism have been previously linked in *Neurospora crassa*.

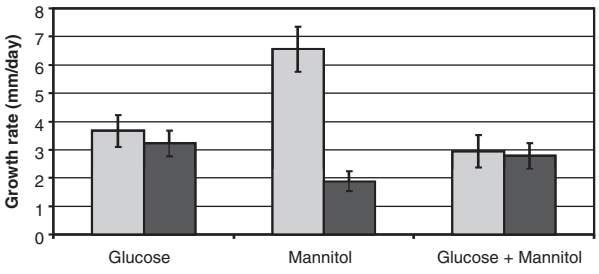

Figure 3. A histogram representing growth rate measurements for *S. nodorum* SN15 and the *Gna1* mutant on Minimal Medium agar plates containing either glucose or mannitol or glucose and mannitol. Plates were grown in darkness at 22°C with radial growth measured every 3 days. Light grey bars represent the wild-type strain and the dark grey bars represent the growth of the *gna1* strain. ($n = 8$, SE bars shown).

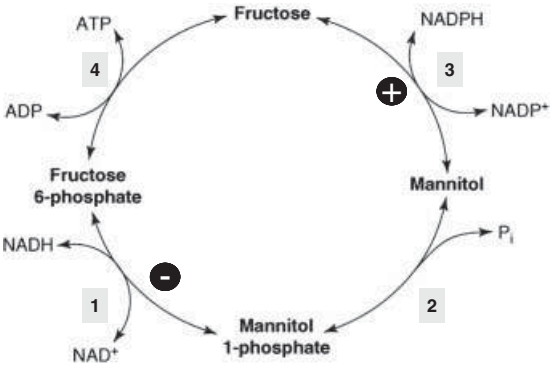

Figure 4. A schematic diagram representing mannitol metabolism. ''+'' symbol indicates that the abundance of that enzyme was up-regulated in the gna1 strain while the ''–'' symbol represents less abundant. 1, Mannitol 1-phosphate dehydrogenase; 2, Mannitol 1-phosphatase; 3, Mannitol dehydrogenase; 4, Hexokinase (adapted from [35]).

Terenzi *et al.* [36] found that a mutant of *N. crassa* lacking cr-1, an adenylate cyclase, was unable to utilise mannitol as a sole carbon source. More recently, Li and Borkovich [37] showed that GPR-4, a G-protein couple receptor was also required for wild-type growth of *N. crassa* on mannitol as a sole carbon source. The same study also confirmed the findings of Terenzi *et al.* on the requirement of cr-1 for mannitol-dependent growth. Growth experiments in this study show that growth of the *gna1* strain on mannitol is slower than it is on glucose, suggesting regulatory similarities for G-protein regulation between *N. crassa* and *S. nodorum* at this level. Previous studies from this laboratory have demonstrated that Mpd1 is critical for both the anabolism and catabolism of mannitol [24, 25]. Mdh1 has only a minor role and appears redundant for the metabolism of mannitol. Consequently, the data above implies that the decreased activity and abundance of Mpd1 in the *gna1* strain results in an inability to use mannitol as a carbon source.

3.3 Gna1 regulates various facets of primary metabolism in *S. nodorum*

Several other proteins identified as being up-regulated in the *gna1* strain are known to either consume NADPH or participate in pathways doing so (Table 1). Fatty acid synthesis (ATP citrate lyase and citrate synthase), ergosterol biosynthesis (farnesyl pyrophosphate synthetase) and nucleotide biosynthesis (GMP synthase) are all processes requiring NADPH. Mannitol dehydrogenase also uses NADPH in the reduction of fructose to mannitol and has been previously linked to NADPH regeneration. However, several reports have since dismissed this postulated role for NAPDH generation in filamentous fungi [25, 35, 38–40]. The pentose phosphate pathway (PPP) is primarily responsible for NAPDH production in *S. nodorum*. Two enzymes from the PPP, 6-phosphogluconate dehydrogenase and glucose-6-phosphate 1-dehydrogenase, were both up-regulated in the absence of Gna1, suggesting increased NADPH synthesis in response to the increased demand discussed above.

It is also significant to note the down-regulation of 3-deoxy-7-phosphoheptulonate synthase (SNOG_02108.2), the first enzyme in the aromatic amino acid biosynthetic pathway. The substrate for this enzyme is erythrose 4-phosphate, an intermediate of the PPP, thus providing a further link between Gna1 regulation and the PPP. Another prominent phenotype of the *gna1* strain is the secretion of significant quantities of tyrosine, phenylalanine and dihydroxyphenylalanine (DOPA) correlating with albinism. Tyrosine and phenylalanine are aromatic amino acids and also intermediates of the DOPA melanin synthetic pathway. The increased levels of tyrosine and phenylalanine (probably due to their lack of incorporation into DOPA) may impose feedback inhibition on 3-deoxy-7-phosphoheptulonate synthase as it is the first committed step in the synthesis of these amino acids [41].

The fate of glucose 6-phosphate is not restricted to NADPH production (Fig. 5). Its metabolism through the PPP can be regulated depending on the physiological status of the cell. The up-regulation of transaldolase and transketolase in the *gna1* strain suggest that glucose 6-phosphate is not solely destined for NADPH production but also for ATP synthesis. This is further supported by the presence of several other enzymes concerned with energy production that are up-regulated in the *gna1* strain, including dihydrolipoamide dehydrogenase (pyruvate decarboxylase complex E3), phosphoglycerate mutase and citrate synthase. It is noted that proteins associated with glycolysis (phosphoglycerate kinase) and the tricarboxylic acid cycle (malate dehydrogenase) were down-regulated in the *gna1* strain, suggesting a pleiotropic effect on metabolic regulation by Gna1. Glucose 6-phosphate is also directly involved in the reactions of two other proteins negatively regulated by Gna1. Phosphoglucomutase is part of the glycogen catabolic pathway and is responsible for the conversion of glucose 1-phosphate to glucose 6-phosphate. Inositol 3-phosphate

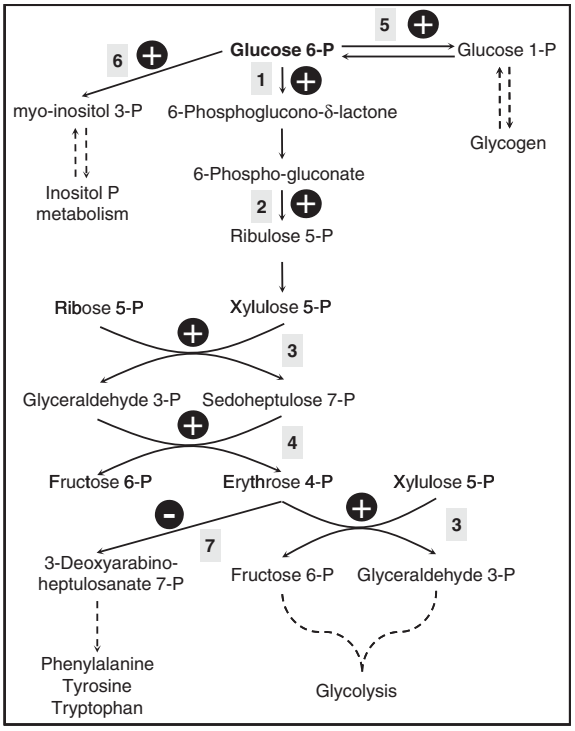

Figure 5. A schematic biochemical pathway outlining the fate of glucose 6-phosphate. "+" symbol indicates that the abundance of that enzyme was up-regulated in the gna1 strain whilst the "−" symbol represents less abundant. 1, Glucose-6-phosphate 1-dehydrogenase; 2, 6-Phosphogluconate dehydrogenase; 3, Transketolase; 4, Transaldolase; 5, Phosphoglucomutase; 6, Inositol-3-phosphate synthase; 7, 3-deoxy-7-phosphoheptulonate synthase

synthase was also up-regulated in the *gna1* strain and it is responsible for catalysing the synthesis of inositol 3-phosphate from glucose 6-phosphate. These results imply that Gna1 signalling has an important regulatory role in determining the fate of glucose 6-phosphate (Fig. 4). Collectively these data suggest, either directly or indirectly, that Gna1 has a regulatory role in various facets of primary metabolism. Metabolomics studies are now ongoing to better understand the impact of Gna1 on primary metabolism.

3.4 Several stress-related proteins are regulated by Gna1

The most strongly down-regulated gene in the mutant is glutaredoxin. Glutaredoxins have glutathione-dependent disulfide reductase activity and limit protein disulfide generated by oxidation of protein sulfhydryl groups by ROS [42]. This mechanism is important for repairing oxidative damage to proteins as well as for regulating the redox state of proteins [42]. Also down-regulated in the *gna1* strain was SNOG_13840.2, a protein sharing very strong similarity to bifunctional catalase-peroxidases. However, previous studies in *S. nodorum* have shown that under *in vitro* conditions, the *gna1* strain does not exhibit increased sensitivity to oxidative stress (Solomon *et al.*, unpublished data).

There were also several down-regulated proteins, which currently have unknown functions, particularly in fungi. SNOG_04306.2 encodes a protein with a glutamine amidotransferase-like (GATase1) domain (Pfam IP: PF00117). The *S. cerevisiae* ortholog (Ydr533c) is up-regulated in response to various stress conditions although the function of SNOG_04306.2 in *S. nodorum* in unclear. Also of interest was SNOG_15275.2, a putative member of the CyanoVirin-N protein family (Pfam ID:PF08881). The anti-viral protein, cyanovirin-N (CV-N) was originally isolated from culture extracts of the cyanobacterium *Nostoc ellipsosporum* [43, 44]. The antiviral activity of CV-N is mediated through high-affinity interactions with the GlcNAc-derived carbohydrate moieties of the HIV envelope, thus impairing virus–cell or cell–cell fusion [44]. The role of these proteins in fungi is largely unknown although it is suspected they are capable of binding various carbohydrates.

3.5 Functional analysis of SNOG_08282

SNOG_08282 was 3.2-fold less abundant in the *gna1* strain implying that Gna1 is a positive regulator. Sequence analysis (BlastP) of SNOG_08282 reveals only weak matches with proteins from other filamentous fungi. A conserved domain analysis of the SNOG_08282 protein sequence revealed the presence of a Rossmann-fold NAD(P)(+)-binding domain. These domains are characteristic of short-chain dehydrogenases, and consequently, SNOG_08282 was re-named *Sch3*.

To functionally characterise *Sch3*, the gene was disrupted by homologous recombination. Three independent mutants were obtained, *S. nodorum sch3-17*, *sch3-24* and *sch3-27*. The phenotype of the *Sch3* mutants growing *in vitro* was indistinguishable from the wild-type along with their ability to utilise a wide variety of carbon sources (Supporting Information Fig. 3). Sporulation of the mutants *in vitro* was also unaffected. The pathogenicity of the mutants was assessed *via* both a detached leaf assay and also a whole-plant spray. Both assays confirmed that the mutants were fully pathogenic with respect to lesion development (Supporting Information Fig. 4). The ability of the *sch3* strains to sporulate was also examined using a latent period assay. A quantitative assessment of the number of pycnidia produced by each of the mutants revealed that *Sch3* is required to complete the pathogenic lifecycle of *S. nodorum* (Fig. 6). The number of pycnidia produced by the *sch3* strains was significantly less than the wild-type or ectopic control. The number of spores within the pycnidia correlated with the number of pycnidia implying that of those pycnidia that do develop, they do appear to fully differentiate into mature structures.

These data confirm the role of *Sch3* in pycnidial development in *S. nodorum* and its down-regulation in the *gna1*

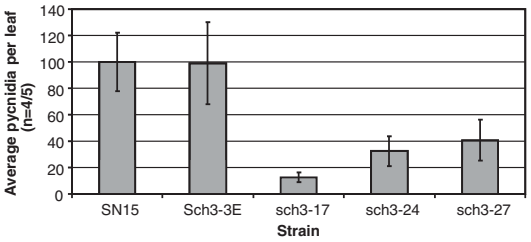

Figure 6. A histogram representing the average number of pycnidia present on wheat leaves infected with strains of *S. nodorum*. ($n = 4/5$, SE bars shown). SN15 is the wild-type *S. nodorum* isolate, Sch3-3E is an ectopic control while sch3-17/24/27 are three independent transformants that have undergone homologous recombination.

mutant implies that *Sch3* is at least partially responsible for the inability of the *gna1* strains to sporulate. It should be noted that several other genes associated with *Gna1* signalling have been identified and characterised with the resulting mutants each harbouring sporulation defects. These data are all contributing to the idea that multiple genes, each under the control of *Gna1*, have varied roles in the developmental stages of the sporulation process including pyncidial initiation (*Mpd1* – mannitol metabolism), establishment of pycnidia (*Sch3* – unknown function) and pycnidial maturation (*Sch1* – unknown function with possible link to secondary metabolism). Studies are now ongoing to determine the role of Sch3 and also Sch1.

4 Concluding remarks

This study has highlighted the significant potential of LC-based proteomics and iTRAQ to analyse the proteomes of pathogenic fungi at a quantitative level. In excess of 1300 proteins were identified with 49 being significantly differentially abundant when comparing the wild-type and *gna1* strains. These differentially abundant proteins highlight the regulatory role of Gna1 on mannitol metabolism, other primary metabolic pathways and asexual sporulation. Several other novel hypothetical proteins were identified, which require further experimentation to deduce their biological roles.

The MS analyses were performed in facilities provided by the Lotterywest State Biomedical Facility-Proteomics node, Western Australian Institute for Medical Research. The Grains Research and Development Corporation is gratefully acknowledged for funding.

The authors have declared no conflict of interest.

5 References

[1] Solomon, P. S., Tan, K. C., Sanchez, P., Cooper, R. M., Oliver, R. P., The disruption of a Gα subunit sheds new light on the pathogenicity of *Stagonospora nodorum* on wheat. *Mol. Plant Microbe Interact.* 2004, *17*, 456–466.

[2] Regenfelder, E., Speelig, T., Hartman, A., Lauenstein, S. *et al.*, G proteins in *Ustilago maydis*: transmission of multiple signals? *EMBO J.* 1997, *16*, 1934–1942.

[3] Fang, E. G. C., Dean, R. A., Site-directed mutagenesis of the magB gene affects growth and development in *Magnaporthe grisea*. *Mol. Plant Microbe Interact.* 2000, *13*, 1214–1227.

[4] Gao, S., Nuss, D. L., Distinct roles for two G protein alpha subunits in fungal virulence, morphology, and reproduction revealed by targeted gene disruption. *Proc. Natl. Acad. Sci. USA* 1996, *93*, 14122–14127.

[5] Gronover, C. S., Kasulke, D., Tudzynski, P., Tudzynski, B., The role of G protein alpha subunits in the infection process of the gray mold fungus *Botrytis cinerea*. *Mol. Plant Microbe Interact.* 2001, *14*, 1293–1302.

[6] Horwitz, B. A., Sharon, A., Lu, S. W., Ritter, V. *et al.*, A G protein alpha subunit from *Cochliobolus heterostrophus* involved in mating and appressorium formation. *Fungal Genet. Biol.* 1999, *26*, 19–32.

[7] Jain, S., Akiyama, K., Mae, K., Ohguchi, T., Takata, R., Targeted disruption of a G protein α subunit gene results in reduced pathogenicity in *Fusarium oxysporum*. *Curr. Genet.* 2002, *41*, 407–413.

[8] Liu, S. H., Dean, R. A., G protein alpha subunit genes control growth, development, and pathogenicity of *Magnaporthe grisea*. *Mol. Plant Microbe Interact.* 1997, *10*, 1075–1086.

[9] Yamagishi, D., Otani, H., Kodama, M., G protein signaling mediates developmental processes and pathogenesis of *Alternaria alternata*. *Mol. Plant Microbe Interact.* 2006, *19*, 1280–1288.

[10] Hane, J. K., Lowe, R. G. T., Solomon, P. S., Tan, K. C. *et al.*, Dothideomycete-plant interactions illuminated by genome sequencing and EST analysis of the wheat pathogen *Stagonospora nodorum*. *Plant Cell* 2007, *19*, 3347–3368.

[11] Solomon, P. S., Lowe, R. G. T., Tan, K.-C., Waters, O. D. C. *et al., Stagonospora nodorum*; cause of Septoria nodorum blotch of wheat. *Mol. Plant Pathol.* 2006, *7*, 147–156.

[12] Brennan, J. P., Murray, G., *Economic Importance of Wheat Diseases in Australia*, NSW Agriculture, Wagga Wagga 1998.

[13] Solomon, P. S., Wilson, T. J. G., Rybak, K., Parker, K. *et al.*, Structural characterisation of the interaction between *Triticum aestivum* and the dothideomycete pathogen *Stagonospora nodorum*. *Eur. J. Plant Pathol.* 2006, *114*, 275–282.

[14] Gronover, C. S., Schorn, C., Tudzynski, B., Identification of *Botrytis cinerea* genes up-regulated during infection and controlled by the G alpha subunit BCG1 using suppression subtractive hybridization (SSH). *Mol. Plant Microbe Interact.* 2004, *17*, 537–546.

[15] Dawe, A. L., Segers, G. C., Allen, T. D., McMains, V. C., Nuss, D. L., Microarray analysis of *Cryphonectria parasitica* G alpha- and G beta gamma-signalling pathways reveals extensive modulation by hypovirus infection. *Microbiology* 2004, *150*, 4033–4043.

[16] Gygi, S. P., Rochon, Y., Franza, B. R., Aebersold, R., Correlation between protein and mRNA abundance in yeast. *Mol. Cell. Biol.* 1999, *19*, 1720–1730.

[17] Tan, K.-C., Heazlewood, J. L., Millar, A. H., Thomson, G. *et al.,* A signaling-regulated, short-chain dehydrogenase of *Stagonospora nodorum* regulates asexual development. *Eukaryot. Cell* 2008, *7*, 1916–1929.

[18] Tan, K.-C., IpCho, S. V. S., Trengove, R. D., Oliver, R. P., Solomon, P. S., Assessing the impact of transcriptomics, proteomics and metabolomics on fungal phytopathology. *Mol. Plant Pathol.* 2009, *10*, 703–715.

[19] Tan, K.-C., Heazlewood, J. L., Millar, A. H., Oliver, R. P., Solomon, P. S., Proteomic identification of extracellular proteins regulated by the Gna1 Gα subunit in *Stagonospora nodorum*. *Mycol. Res.* 2009, *113*, 523–531.

[20] Vitali, B., Wasinger, V., Brigidi, P., Guilhaus, M., A proteomic view of Bifidobacterium infantis generated by multidimensional chromatography coupled with tandem mass spectrometry. *Proteomics* 2005, *5*, 1859–1867.

[21] Ross, P. L., Huang, Y. N., Marchese, J. N., Williamson, B. *et al.,* Multiplexed protein quantitation in *Saccharomyces cerevisiae* using amine-reactive isobaric tagging reagents. *Mol. Cell. Proteomics* 2004, *3*, 1154–1169.

[22] Kuzyk, M. A., Ohlund, L. B., Elliott, M. H., Smith, D. *et al.,* A comparison of MS/MS-based, stable-isotope-labeled, quantitation performance on ESI-quadrupole TOF and MALDI-TOF/TOF mass spectrometers. *Proteomics* 2009, *9*, 3328–3340.

[23] Yang, Y., Zhang, S., Howe, K., Wilson, D. B. *et al.,* A comparison of nLC-ESI-MS/MS and nLC-MALDI-MS/MS for GeLC-based protein identification and iTRAQ-based shotgun quantitative proteomics. *J. Biomol. Tech.* 2007, *18*, 226–237.

[24] Solomon, P. S., Tan, K.-C., Oliver, R. P., Mannitol 1-phosphate metabolism is required for sporulation *in planta* of the wheat pathogen *Stagonospora nodorum*. *Mol. Plant Microbe Interact.* 2005, *18*, 110–115.

[25] Solomon, P. S., Waters, O. D. C., Joergens, C. I., Lowe, R. G. T. *et al.,* Mannitol is required for asexual sporulation in the wheat pathogen *Stagonospora nodorum* (glume blotch). *Biochem. J.* 2006, *399*, 231–239.

[26] Lu, H., Yang, Y., Allister, E. M., Wijesekara, N., Wheeler, M. B., The identification of potential factors associated with the development of type 2 diabetes: a quantitative proteomics approach. *Mol. Cell. Proteomics* 2008, *7*, 1434–1451.

[27] Schneider, T., Schellenberg, M., Meyer, S., Keller, F. *et al.,* Quantitative detection of changes in the leaf-mesophyll tonoplast proteome in dependency of a cadmium exposure of barley (*Hordeum vulgare* L.). *Plant Proteomics* 2009, *9*, 2668–2677.

[28] Solomon, P. S., Rybak, K., Trengove, R. D., Oliver, R. P., Investigating the role of calcium/calmodulin-dependent protein signalling in *Stagonospora nodorum*. *Mol. Microbiol.* 2006, *62*, 367–381.

[29] Solomon, P. S., Thomas, S. W., Spanu, P., Oliver, R. P., The utilisation of di/tripeptides by *Stagonospora nodorum* is dispensable for wheat infection. *Physiol. Mol. Plant Pathol.* 2003, *63*, 191–199.

[30] Noeldner,P. K. M., Coleman, M. J., Faulks, R., Oliver, R. P., Purification and characterization of mannitol dehydrogenase from the fungal tomato pathogen *Cladosporium fulvum* (syn *Fulvia fulva*). *Physiol. Mol. Plant Pathol.* 1994, *45*, 281–289.

[31] Smith, P. K., Krohn, R. I., Hermanson, G. T., Maliia, A. K. *et al.,* Measurement of protein using bicinchoninic acid. *Anal. Biochem.* 1985, *150*, 76–85.

[32] Wu, W. W., Wang, G., Baek, S. J., Shen, R.-F., Comparative study of three proteomic quantitative methods, DIGE, cICAT, and iTRAQ, using 2D gel- or LC-MALDI TOF/TOF. *J. Prot. Res.* 2006, *5*, 651–658.

[33] Washburn, M. P., Wolters, D., Yates, J. R., Large-scale analysis of the yeast proteome by multidimensional protein identification technology. *Nat. Biotech.* 2001, *19*, 242–247.

[34] Gagne, J. P., Ethier, C., Gagne, P., Mercier, G. *et al.,* Comparative proteome analysis of human epithelial ovarian cancer. *Proteome Sci.* 2007, *5*, 16.

[35] Solomon, P. S., Waters, O. D. C., Oliver, R. P., Decoding the enigmatic mannitol in filamentous fungi. *Trends Microbiol.* 2007, *15*, 257–262.

[36] Terenzi, H. F., Jorge, J. A., Roselino, J. E., Migliorini, R. H., Adenylyl cyclase deficient cr-1 (Crisp) mutant of *Neurospora crassa*: cyclic AMP-dependent nutritional deficiencies. *Arch. Microbiol.* 1979, *123*, 251–258.

[37] Li, L., Borkovich, K. A., GPR-4 is a predicted G-protein-coupled receptor required for carbon source-dependent asexual growth and development in *Neurospora crassa*. *Eukaryot. Cell* 2006, *5*, 1287–1300.

[38] Velez, H., Glassbrook, N. J., Daub, M. E., Mannitol metabolism in the phytopathogenic fungus *Alternaria alternata*. *Fungal Genet. Biol.* 2006, *44*, 258–268.

[39] Ruijter, G. J. G., Bax, M., Patel, H., Flitter, S. J. *et al.,* Mannitol is required for stress tolerance in *Aspergillus niger* conidiospores. *Eukaryot. Cell* 2003, *2*, 690–698.

[40] Singh, M., Scrutton, N. S., Scrutton, M. C., NADPH generation in *Aspergillus nidulans*: is the mannitol cycle involved? *J. Gen. Microbiol.* 1988, *134*, 643–654.

[41] Hartmann, M., Schneider, T. R., Pfeil, A., Heinrich, G. *et al.,* Evolution of feedback-inhibited α/β barrel isoenzymes by gene duplication and a single mutation. *Proc. Natl. Acad. Sci. USA* 2003, *100*, 862–867.

[42] Sato, I., Shimizu, M., Hoshino, T., Takaya, N., The glutathione system of *Aspergillus nidulans* involves a fungus-specific glutathione s-transferase. *J. Biol. Chem.* 2009, *284*, 8042–8053.

[43] Percudani, R., Montanini, B., Ottonello, S., The anti-HIV cyanovirin-N domain is evolutionarily conserved and occurs as a protein module in eukaryotes. *Proteins: Structure, FunctionBioinformatics* 2005, *60*, 670–678.

[44] Boyd, M. R., Gustafson, K. R., McMahon, J. B., Shoemaker, R. H. *et al.,* Discovery of cyanovirin-N, a novel human immunodeficiency virus- inactivating protein that binds viral surface envelope glycoprotein gp120: potential applications to microbicide development. *Antimicrob. Agents Chemother.* 1997, *41*, 1521–1530.

